

## Supporting Information

### Electrolyte Solvation Structure Manipulation Enables Safe and Stable Aqueous

### Sodium ion battery

Huasheng Ao,<sup>a</sup> Chunyuan Chen,<sup>b</sup> Zhiguo Hou,<sup>a</sup> Wenlong Cai,<sup>a</sup> Mengke Liu,<sup>a</sup> Yueang Jin,<sup>a</sup> Xin Zhang,<sup>b</sup> Yongchun Zhu,<sup>\*a</sup> and Yitai Qian<sup>a</sup>

<sup>a</sup>Department of Applied Chemistry, Hefei National Laboratory for Physical Science at Microscale, University of Science and Technology of China 96 JinZhai Road, 230026, Hefei, China.

<sup>b</sup>State Key Laboratory of Chemical Resource Engineering, Beijing Advanced Innovation Center for Soft Matter Science and Engineering, Beijing University of Chemical Technology, Beijing 100029, China

\* Corresponding author. E-mail: ychzhu@ustc.edu.cn.

## Experimental section

### Material synthesis

All chemicals were obtained from Sinopharm Chemical Reagent Co. Ltd (China) and were used without further treatment. The  $\text{Na}_3\text{V}_2(\text{PO}_4)_3/\text{C}$  cathode material were prepared by a sol-gel method. Typically, 2 mmol  $\text{NH}_4\text{VO}_3$  was dissolved in 100 mL distilled water under vigorous stirring at 80 °C to get a yellow solution. The stoichiometric amount of  $\text{CH}_3\text{COONa}\cdot 3\text{H}_2\text{O}$ 、 $\text{NH}_4\text{H}_2(\text{PO}_4)_3$  and 2 mmol citric acid were added in solution and vigorous stirring to evaporate water, then dried in vacuum at 60 °C overnight. The obtained precursor was ground and pre-treated at 400 °C for 5 h, followed by sintering at 750 °C under  $\text{Ar}/\text{H}_2(95/5$  in volume) atmosphere obtain the final  $\text{Na}_3\text{V}_2(\text{PO}_4)_3/\text{C}$  composite. The material Nickel based Prussian blue was synthesized through a co-precipitation reaction. Firstly, analytical pure 2 mmol  $\text{NiSO}_4$  was dissolved in 100 mL deionized water (solution A) and 2 mmol  $\text{Na}_4\text{Fe}(\text{CN})_6$  was dissolved in 100 mL water (solution B). Then solution A and B were co-injected into 100 mL water in which dissolved 10 g  $\text{Na}_2\text{SO}_4$  with a speed of 0.5 mL per minute under magnetic stirring. After aged 12 h, the white precipitation was filtered washed with water and ethanol three time. And then the product was dried under vacuum at room temperature for 10 h. The  $\text{NaTi}_2(\text{PO}_4)_3/\text{C}$  anode material were synthesized with a synchronous carbon complex process. Firstly, the stoichiometric amount of tetrabutyl titanate,  $\text{NH}_4\text{H}_2(\text{PO}_4)_3$  and edetate disodium were ground with water and ethanol at 500 rpm for 5 h. Subsequently, the precursor was pre-treated under Ar atmosphere at 400 °C for 5 h, and annealing at 750 °C for 10 h under  $\text{Ar}/\text{H}_2$  (95/5 in volume) atmosphere. Finally, The  $\text{NaTi}_2(\text{PO}_4)_3/\text{C}$  composite were obtained.

### Electrolyte preparation and characterization

The four kinds of electrolytes were prepared by dissolving one or more appropriate amounts of sodium perchlorate, urea and N,N-dimethylformamide(DMF) in high-purity water (Millipore Milli-Q) at 40 °C under stirring. The superconcentrate  $\text{NaClO}_4$  solution (called as Na- $\text{H}_2\text{O}$ ) was made up of  $\text{NaClO}_4$  and  $\text{H}_2\text{O}$  with the molar ratio of 1:3, The sodium perchlorate,  $\text{H}_2\text{O}$  and urea was compounded with the molar ratio of 1:2:2 (called as Na- $\text{H}_2\text{O}$ -urea), and the sodium perchlorate,  $\text{H}_2\text{O}$ , N,N-dimethylformamide(DMF) was mixed with the molar ratio of 1:2:1 to form the third electrolyte(called as Na- $\text{H}_2\text{O}$ -DMF),the fourth electrolyte (called as Na- $\text{H}_2\text{O}$ -urea-DMF) was prepared by adding urea into the third electrolyte with the molar ratio of 1:2:2:1. All the electrolytes were degassed with  $\text{N}_2$  for 1 h to remove dissolved  $\text{O}_2$  before use. The conductivity of electrolytes were tested by DDS-307A Conductivity Meters (Leici Shanghai) at different temperature. The phase transformation of electrolytes were

provided by the Differential Scanning Calorimeter (DSC Q2000) over a temperature range of -50 to 50 °C. Raman spectra were recorded on a HORIBA LabRAM HR Evolution Invia Raman spectrometer, with an excitation laser wavelength of 532 nm. FTIR spectra were obtained on Thermofisher Nicolet 6700 FTIR spectrometer.  $^1\text{H}$  and  $^{23}\text{Na}$ -NMR spectra were measured on a Bruker AVANCE AV400 NMR spectrometer. Samples were analysed at  $25 \pm 0.1$  °C.

### **Material characterization**

X-ray powder diffraction (XRD) patterns of the products and the electrodes at different charge/discharge states were recorded on a Philips X'pert X-ray diffractometer with  $\text{Cu K}\alpha$  radiation ( $\lambda=1.54182$  Å) at a scan rate of  $0.008842^\circ\text{s}^{-1}$  and Raman spectroscopy is performed by a JYLABRAM-HR Confocal Laser Micro-Raman spectrometer at 532 nm. The morphologies of the samples are characterized on scanning electron microscopy (SEM, JEOL-JSM-6700F), transmission electron microscopy (TEM, Hitachi H7650) and high resolution transmission electron microscopy (HRTEM, JEM-2100F). The carbon content was determined using an elemental analyzer (Vario EL III) in a pure oxygen atmosphere. The thermogravimetric analysis (TGA) of NVP/C and NTP/C composite were performed using the TGA Q5000 IR thermogravimetric analyzer under an air atmosphere. The V ion concentration in the electrolyte of the full cell was analyzed and determined by Inductive Coupled Plasma Emission Spectrometer-Atomic Emission Spectroscopy (ICP-AES, Optima 7300DV). X-ray photoelectron spectroscopy (XPS) is collected on the ESCALAB 250 spectrometer (Perkin-Elmer) with a Kratos Analytical spectrometer and a monochromatic  $\text{Al K}\alpha$  (1486.6 eV) X-ray source. The all samples were recovered from full aqueous Na-ion cell in 2016 coin cell after electrochemical cycles. The NTP electrodes were rinsed by NMP solution three times and then dried under vacuum for an hour before XPS measurement. The spectrum is calibrated using  $\text{C1s}$  spectrum, and the standard binding energy is 284.6 eV.

### **Electrochemical measurements**

Electrochemical properties of NVP/C and NTP/C electrodes were measured using a three-electrode cell setup. In three-electrode cell, a large piece of pure Pt sheet and an  $\text{Ag/AgCl}$  electrode (0.197V vs. SHE) served as counter and reference electrodes, respectively. The working electrode was prepared by mixing the active material, super P carbon black and polyvinylidene fluoride (PVDF) binder with a weight ratio of 80:10:10 in N-methyl-2-pyrrolidinone (NMP) to make slurries coating on a stainless-steel mesh (100 mesh) with about  $1\text{ cm}^2$  area, then the as-prepared electrodes were dried at 80 °C for 10 h in a vacuum oven, and pressed at a pressure of 15 MPa using a

manual hydraulic press. The typical loadings of the active materials of electrodes was 4-6 mg cm<sup>-2</sup>. The 2032 coin type aqueous Na-ion full cells were assembled using a NaTi<sub>2</sub>(PO<sub>4</sub>)<sub>3</sub> anode and a Na<sub>3</sub>V<sub>2</sub>(PO<sub>4</sub>)<sub>3</sub> cathode. Cyclic voltammetry (CV) and linear sweep voltammetry (LSV) was performed on a CHI 660D electrochemical workstation (Shanghai). Galvanostatic charging–discharging tests were carried out on a LAND cyler (Wuhan Kingnuo Electronic Co., China) at room temperature.

### **Computational method**

Geometry of Na complex was optimized by the global-hybrid meta-GGA density functional M08-HX<sup>[1]</sup> with basis set 6-31G\*. Ultrafine integration grids are used in the calculation. The effect of the surrounding environment was included by the SMD solvation model<sup>[2]</sup> using DMF ( $\epsilon = 37.219$ ) as the solvent. The quantum mechanical calculations were carried out with Gaussian 09 program.<sup>[3]</sup>

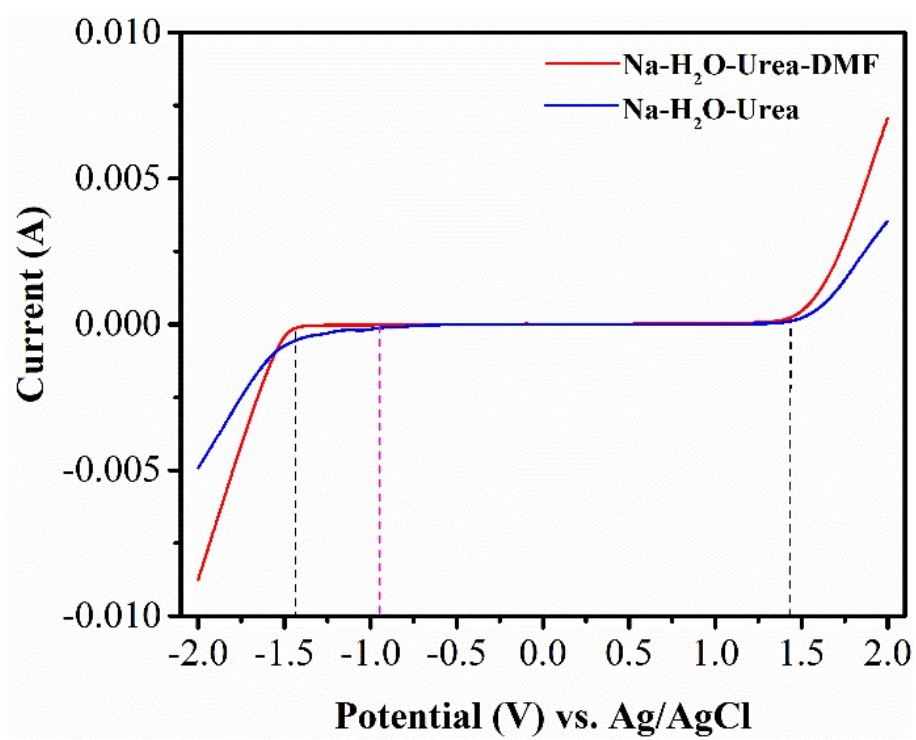


**Figure S1.** Linear sweep voltammetry profiles collected at  $1 \text{ mV s}^{-1}$  for Na-H<sub>2</sub>O-Urea and Na-H<sub>2</sub>O-Urea-DMF electrolytes

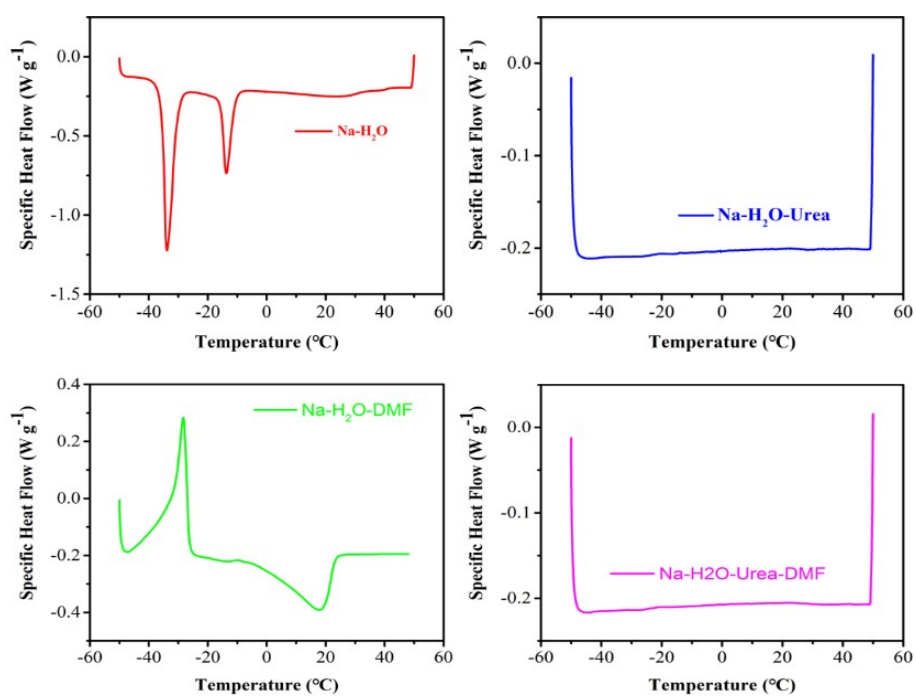


**Figure S2.** Differential scanning thermograms of a) Na-H<sub>2</sub>O, b) Na-H<sub>2</sub>O-Urea, c) Na-H<sub>2</sub>O-DMF, and d) Na-H<sub>2</sub>O-Urea-DMF.



**Figure S3.** The digital photograph of state of different electrolytes at 50°C, 25°C and -40°C.

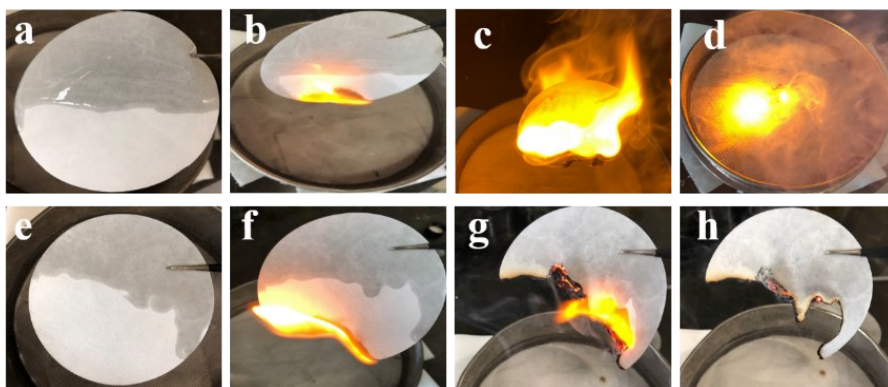


**Figure S4.** The digital photograph of process of electrolytes combustion. a-d) Na-H<sub>2</sub>O-DMF, e-f) Na-H<sub>2</sub>O-Urea-DMF.

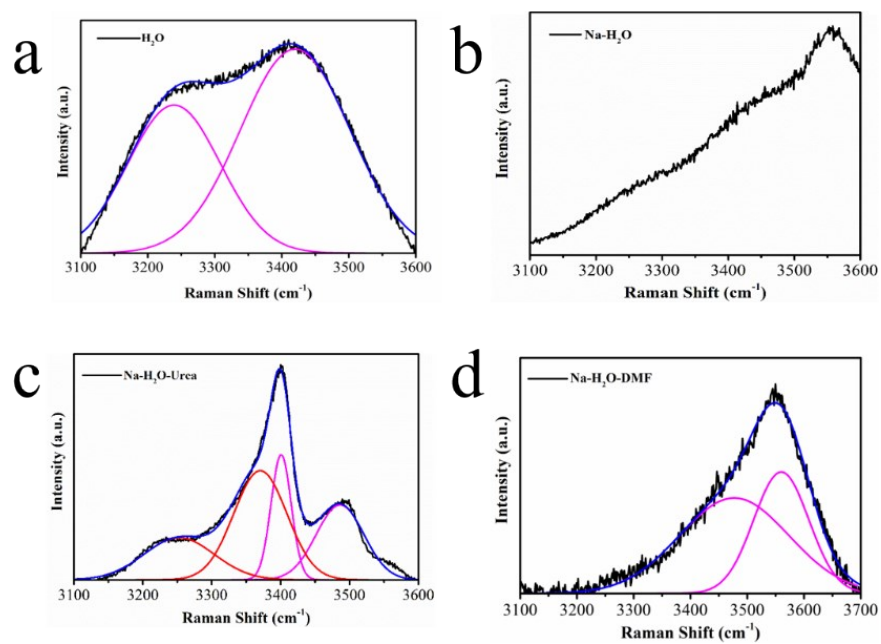


**Figure S5.** O-H or N-H stretching modes in Raman spectra for different electrolytes.

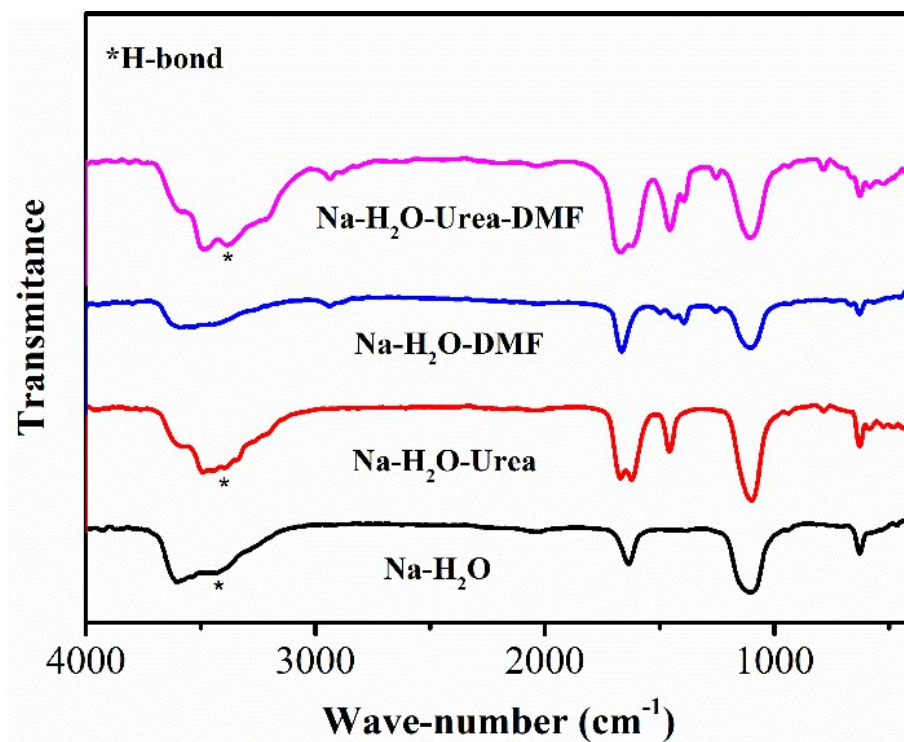


**Figure S6.** FT-IR spectras of Na-H<sub>2</sub>O, Na-H<sub>2</sub>O-Urea, Na-H<sub>2</sub>O-DMF and Na-H<sub>2</sub>O-Urea-DMF.

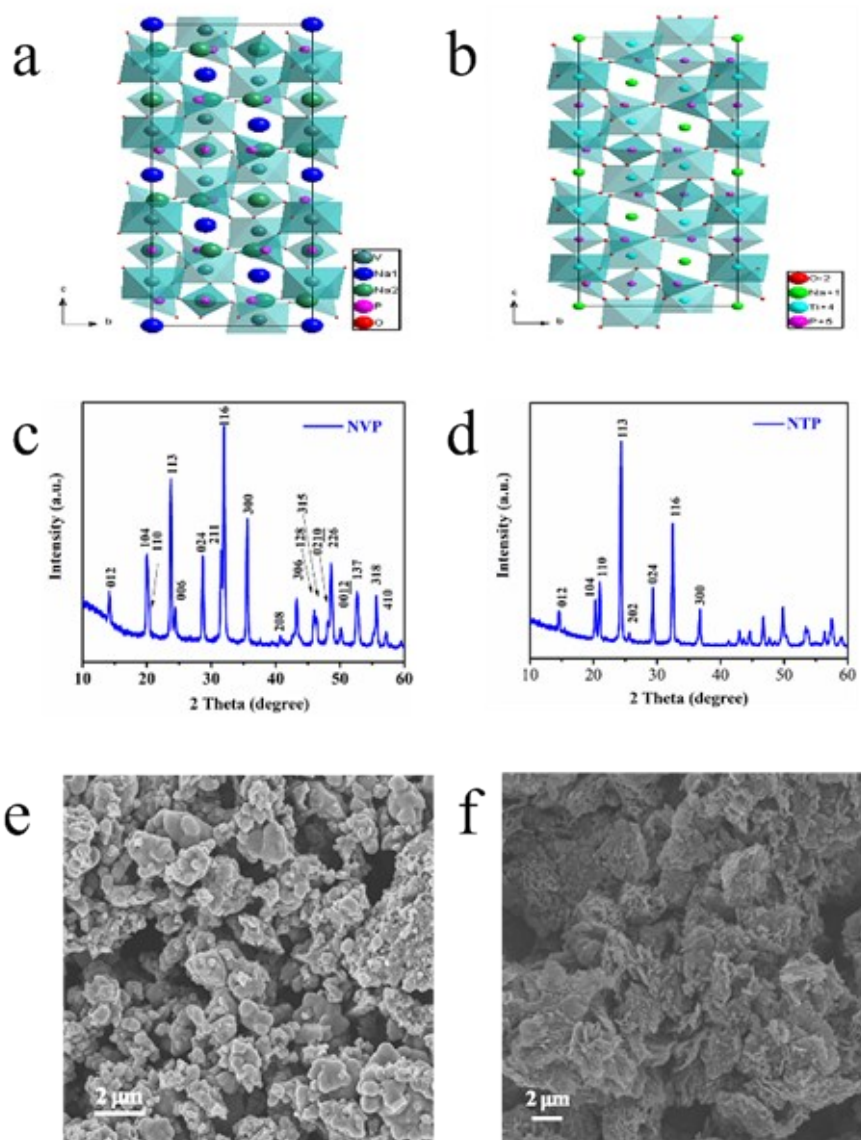


**Figure S7. Materials.** (a, b) crystal structures of NVP and NTP. (c, d) XRD pattern for NVP/C and NTP/C composite. (e, f) SEM images of NVP/C and NTP/C composite with a scale bar of 2  $\mu\text{m}$ .

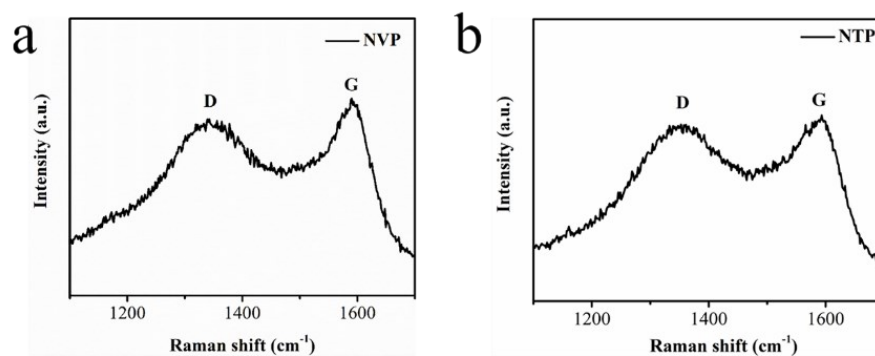


**Figure S8.** The NVP/C and NTP/C samples (a, b) Raman spectra.

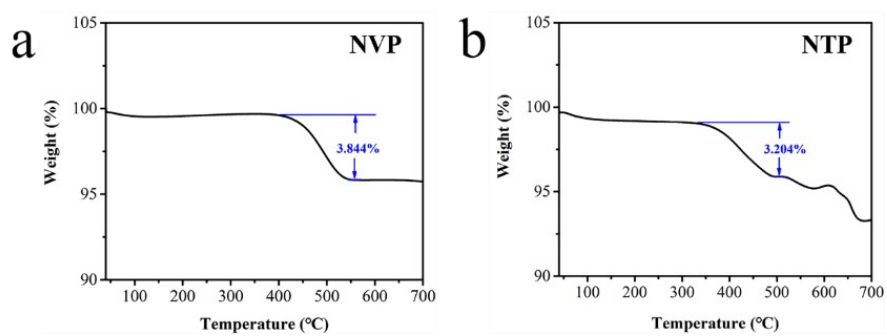


**Figure S9.** The NVP/C and NTP/C samples (a, b) TG curves.

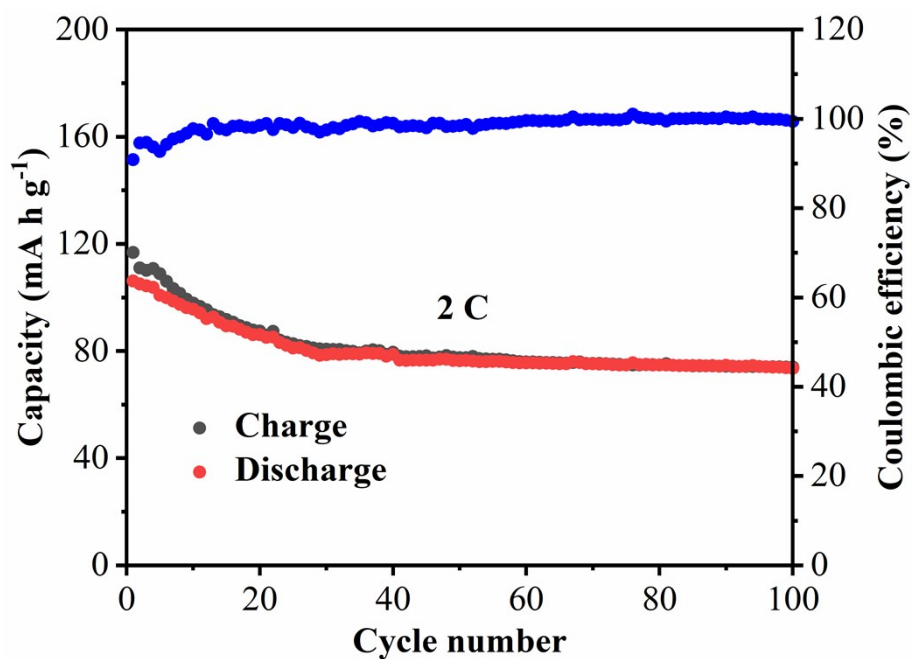


**Figure S10.** Cycle performance of NVP electrode at 2 C with 1 M NaClO<sub>4</sub> in EC:DEC solution.

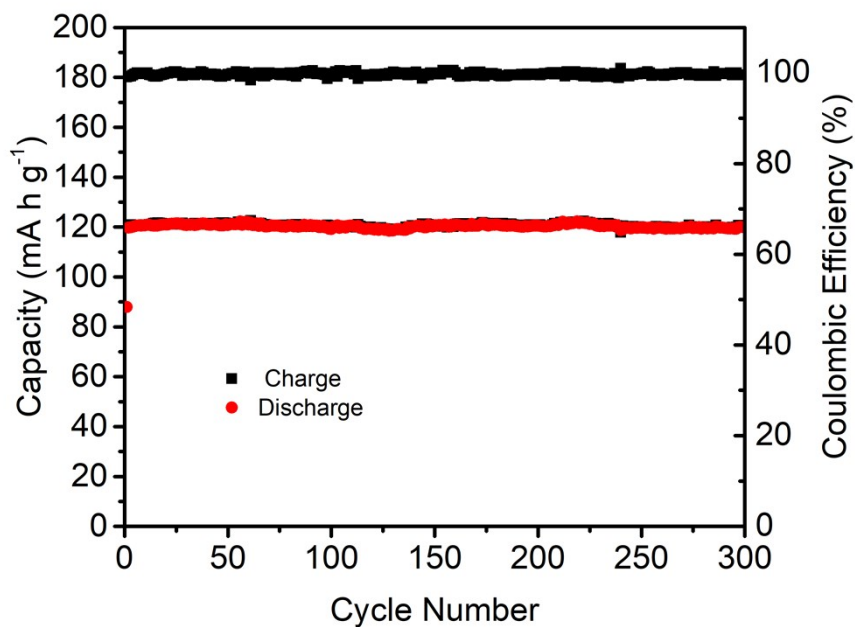


**Figure S11.** Cycle performance of NTP electrode at 1 C with 1 M NaClO<sub>4</sub> in EC:DEC solution.

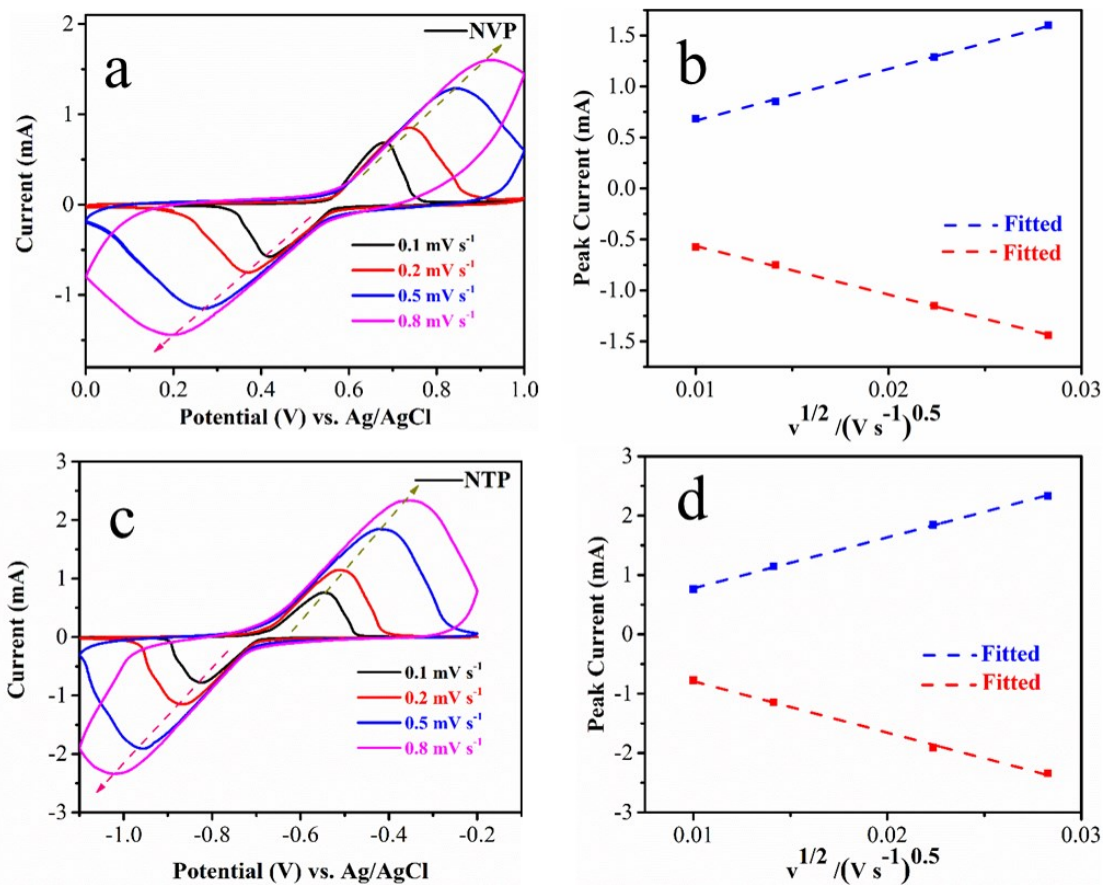


**Figure S12.** (a, c) CV curves of the NVP (e) and NTP (g) aqueous half cell at various scan rates. (b, d) The corresponding linear relationship between the peak current with the square root of scan rate and the fitted lines.

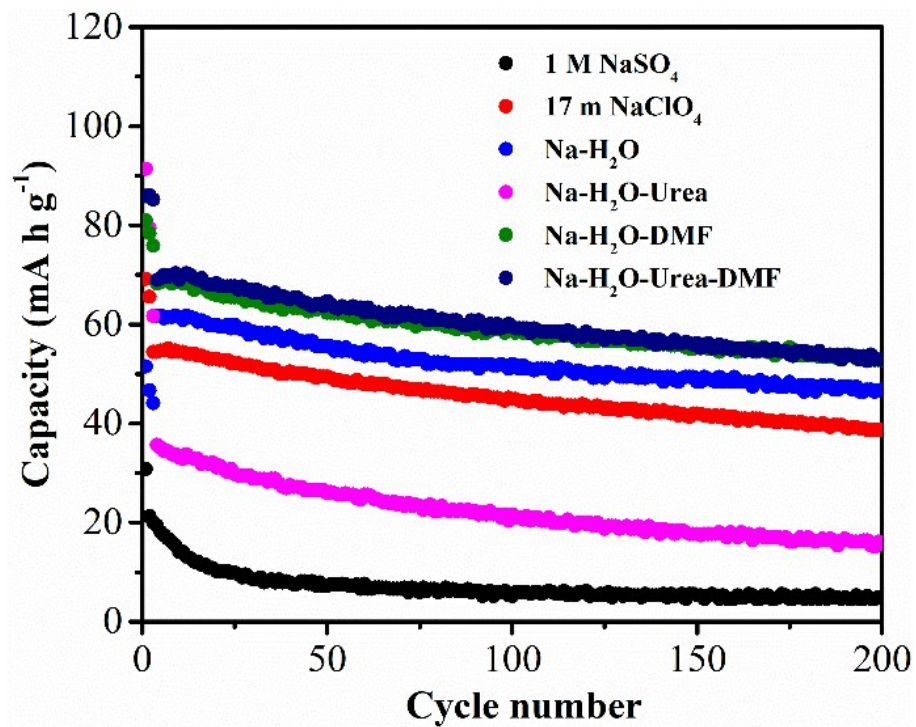


**Figure S13.** The cycle performance of NVP/C//NTP/C full cell in different electrolytes.

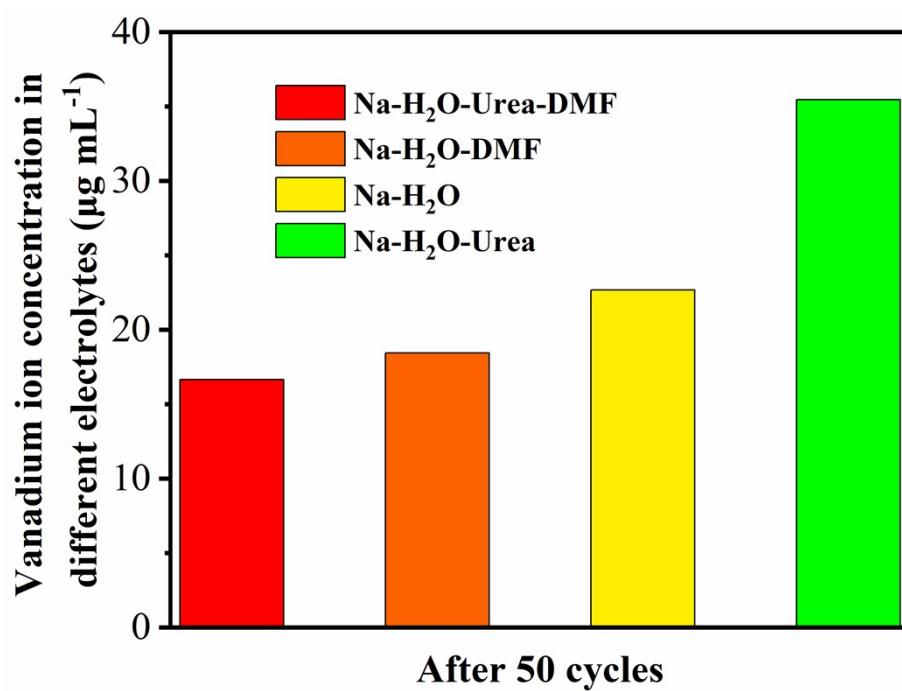


**Figure S14.** The V-ion concentrations in NaClO<sub>4</sub> solution, Na-H<sub>2</sub>O-DMF, Na-H<sub>2</sub>O-Urea and Na-H<sub>2</sub>O-Urea-DMF electrolyte of NVP//NTP full cell after 50 cycles.

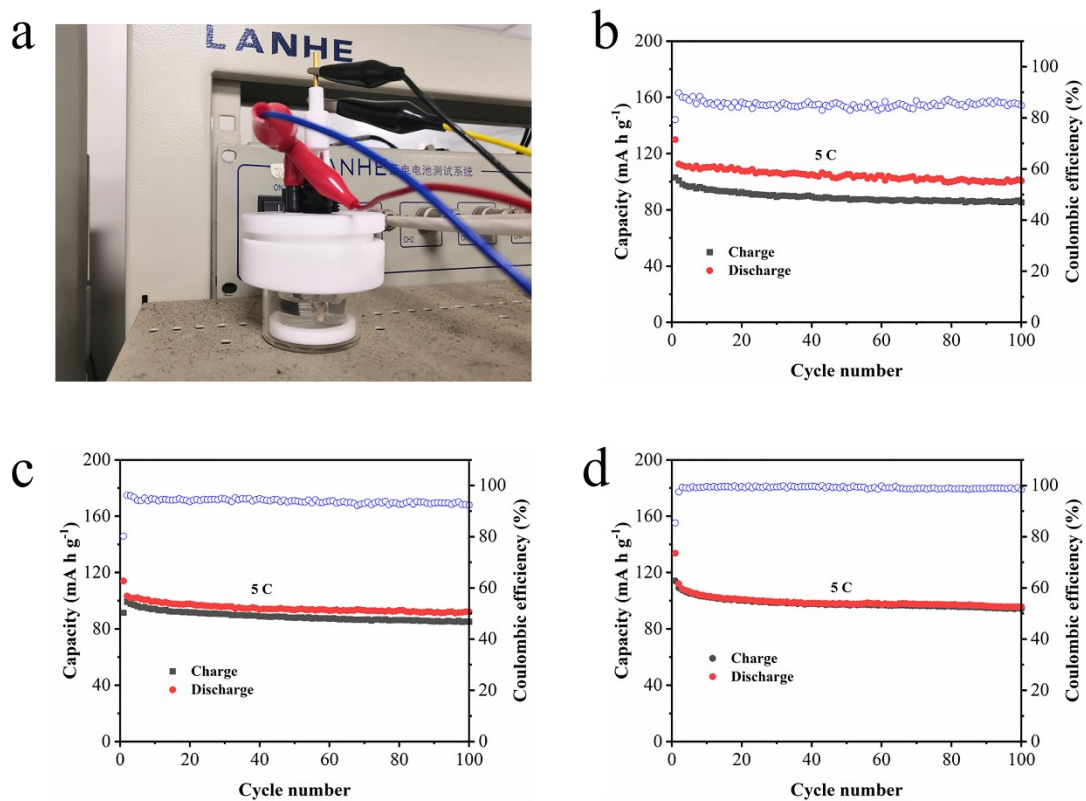


**Figure S15.** (a) Schematic diagram of half-cell test device. (b-d) The cycle performance of NTP anode at 5 C in 1 M Na<sub>2</sub>SO<sub>4</sub>, 17 m NaClO<sub>4</sub>, and Na-H<sub>2</sub>O-Urea-DMF solution, respectively.

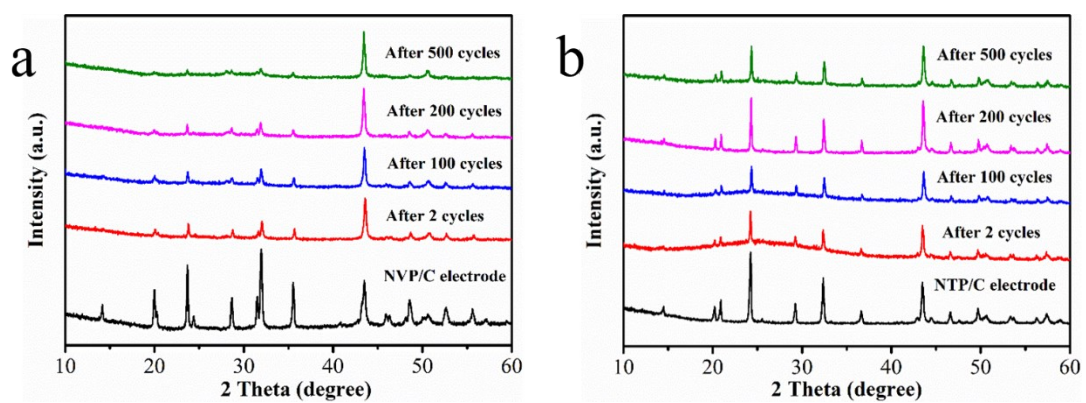


**Figure S16.** The XRD patterns of NVP/C (a) and NTP/C (b) before and after cycles.

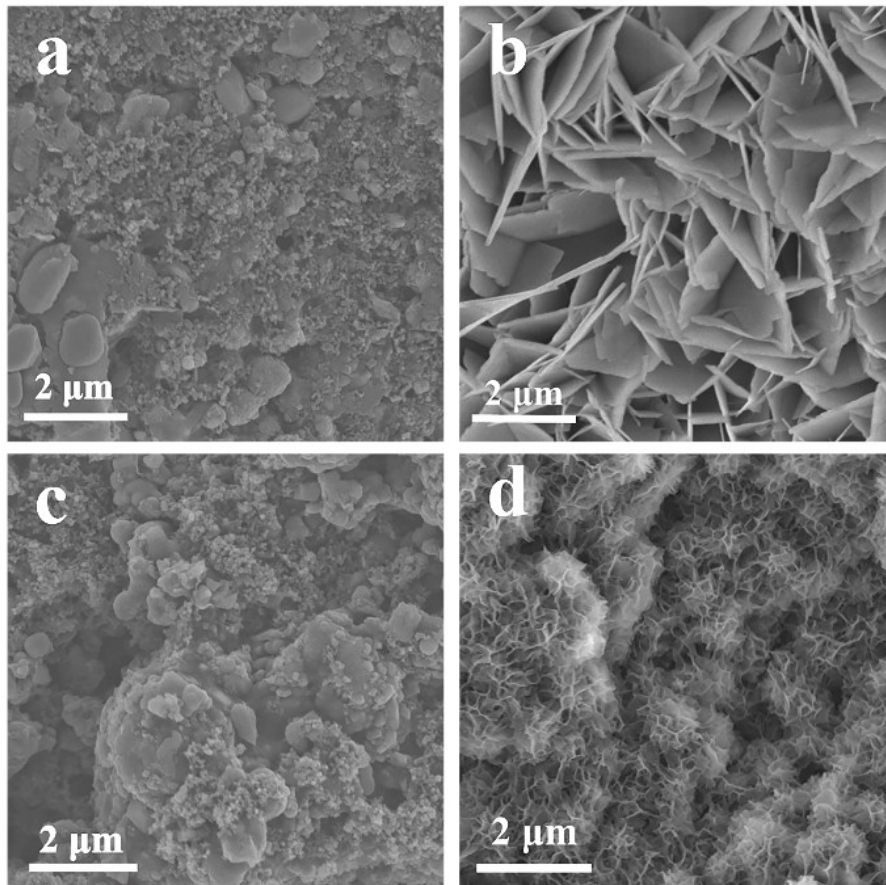


**Figure S17.** The SEM images of NVP/C and NTP/C before and after 500 cycles.

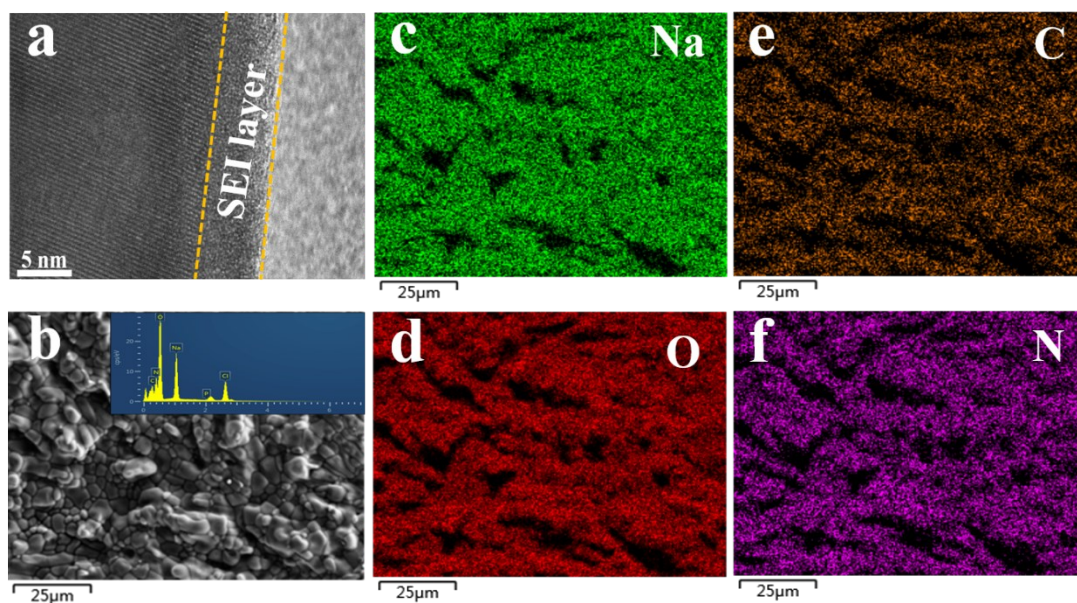


**Figure S18.** (a, b) TEM and SEM images of NTP electrode after 30 cycles in Na-H<sub>2</sub>O-Urea-DMF electrolyte. (c-f) The distribution of Na, C, O and N elements on the surface of NTP electrode after 30 cycles in Na-H<sub>2</sub>O-Urea-DMF electrolyte.

**Table S1 the hydrogen bond length in Na complex at M08-HX/6-31G\*/SMD level**

	H1@H <sub>2</sub> O1...	H2@Urea1	H2@H <sub>2</sub> O2...	
	H2@H <sub>2</sub> O1...	O@Urea1	...	O@Urea2
	N1@Urea2		O@H <sub>2</sub> O2	O2@ClO <sub>4</sub> <sup>-</sup>
<b>Bond length (Å)</b>	<b>2.127</b>	<b>1.919</b>	<b>1.920</b>	<b>1.878</b>
				<b>1.988</b>

**Table S2 the contents carbon measured by elemental analyzer**

<b>Materials</b>	<b>Contents of carbon (%)</b>
NVP/C	3.445
NTP/C	3.968

**Table S3 (ICP-AES) analysis of V in different electrolyte at pristine state, after 50 cycles and after 100 cycles.**

<b>Electrolyte</b>	<b>The concentration of V-ion (µg mL<sup>-1</sup>)</b>		
	<b>pristine</b>	<b>after 50 cycles</b>	<b>after 100 cycles</b>
Na-H <sub>2</sub> O-Urea-DMF	0.05	16.65	20.12
1 M Na <sub>2</sub> SO <sub>4</sub>	0.075	60.68	72.34

**Table S4 the cycle performance of NVP/NTP full cell in aqueous electrolyte in reported work.**

<b>current density</b>	<b>initial capacity</b>	<b>cycle number</b>	<b>capacity retention</b>	<b>ref</b>
	(mAh g <sup>-1</sup> )			
10 A g <sup>-1</sup>	60	50	50%	[4]
10 C	22	100	~100%	[5]
10 C	68	100	86%	This work

**Table S5 (ICP-AES) analysis of V-ion in different electrolyte at after 50 cycles.**

<b>Electrolyte</b>	Na-H <sub>2</sub> O-Urea-DMF	Na-H <sub>2</sub> O-DMF	Na-H <sub>2</sub> O-Urea	Na-H <sub>2</sub> O
<b>The concentration</b>	16.65	18.44	35.46	22.68

of V-ion ( $\mu\text{g mL}^{-1}$ )				
------------------------------------	--	--	--	--

## References

- [1] a) Y. Zhao, D. G. Truhlar, *Theor. Chem. Acc.* **2008**, *120*, 215; b) Y. Zhao, D. G. Truhlar, *Acc. Chem. Res.* **2008**, *41*, 157.
- [2] A. V. Marenich, C. J. Cramer, D. G. Truhlar, *J. Phys. Chem. B* **2009**, *113*, 6378.
- [3] M. J. T. Frisch, G. W.; Schlegel, H. B.; Scuseria, G. E.; Robb, M. A.; Cheeseman, J. R.; Scalmani, G.; Barone, V.; Mennucci, B.; Petersson, G. A.; Nakatsuji, H.; Caricato, M.; Li, X.; Hratchian, H. P.; Izmaylov, A. F.; Bloino, J.; Zheng, G.; Sonnenberg, J. L.; Hada, M.; Ehara, M.; Toyota, K.; Fukuda, R.; Hasegawa, J.; Ishida, M.; Nakajima, T.; Honda, Y.; Kitao, O.; Nakai, H.; Vreven, T.; Montgomery, Jr., J. A.; Peralta, J. E.; Ogliaro, F.; Bearpark, M.; Heyd, J. J.; Brothers, E.; Kudin, K. N.; Staroverov, V. N.; Kobayashi, R.; Normand, J.; Raghavachari, K.; Rendell, A.; Burant, J. C.; Iyengar, S. S.; Tomasi, J.; Cossi, M.; Rega, N.; Millam, J. M.; Klene, M.; Knox, J. E.; Cross, J. B.; Bakken, V.; Adamo, C.; Jaramillo, J.; Gomperts, R.; Stratmann, R. E.; Yazyev, O.; Austin, A. J.; Cammi, R.; Pomelli, C.; Ochterski, J. W.; Martin, R. L.; Morokuma, K.; Zakrzewski, V. G.; Voth, G. A.; Salvador, P.; Dannenberg, J. J.; Dapprich, S.; Daniels, A. D.; Farkas, Ö.; Foresman, J. B.; Ortiz, J. V.; Cioslowski, J.; Fox, D. J., *Gaussian Inc* **2009**.
- [4] Q. Zhang, C. Liao, T. Zhai, H. Li, *Electrochimica Acta* **2016**, *196*, 470.
- [5] H. Zhang, B. Qin, J. Han, S. Passerini, *ACS Energy Lett.* **2018**, *3*, 1769.